nature ecology & evolution

ARTICLES

https://doi.org/10.1038/s41559-019-0839-9

The origin and maintenance of metabolic allometry in animals

Craig R. White[1,2*], Dustin J. Marshall[2], Lesley A. Alton[1,2], Pieter A. Arnold[1,3], Julian E. Beaman[1], Candice L. Bywater[2,4], Catriona Condon[5], Taryn S. Crispin[1], Aidan Janetzki[1], Elia Pirtle[4], Hugh S. Winwood-Smith[1], Michael J. Angilletta Jr[5], Stephen F. Chenoweth[1], Craig E. Franklin[1], Lewis G. Halsey[6], Michael R. Kearney[4], Steven J. Portugal[7] and Daniel Ortiz-Barrientos[1]

Organisms vary widely in size, from microbes weighing 0.1 pg to trees weighing thousands of megagrams — a 10^{21}-fold range similar to the difference in mass between an elephant and the Earth. Mass has a pervasive influence on biological processes, but the effect is usually non-proportional; for example, a tenfold increase in mass is typically accompanied by just a four- to sevenfold increase in metabolic rate. Understanding the cause of allometric scaling has been a long-standing problem in biology. Here, we examine the evolution of metabolic allometry in animals by linking microevolutionary processes to macroevolutionary patterns. We show that the genetic correlation between mass and metabolic rate is strong and positive in insects, birds and mammals. We then use these data to simulate the macroevolution of mass and metabolic rate, and show that the interspecific relationship between these traits in animals is consistent with evolution under persistent multivariate selection on mass and metabolic rate over long periods of time.

Animals expend energy to survive, forage, grow and reproduce, and the processes that cause variation in metabolic rate (R_m) have fascinated biologists for over a century[1–11]. R_m values integrate many organismal functions[12] and relate to several traits that enhance fitness (for example, social dominance, offspring growth and lifetime reproductive success[8,13–15]). Because energy turnover varies according to size, measurements of R_m and body mass (M) are usually strongly correlated. Among species of birds and mammals, for example, more than 94% of the variance in R_m can be explained by M alone[16–18]. Surprisingly, however, R_m is not linearly proportional to M; instead, R_m is proportional to M^b, where b is typically less than one[6,9], especially for the resting R_m and daily mean R_m of free-living animals[19]; b is often higher and can approach isometry ($b = 1$) for maximally active animals[7]. Mechanistic hypotheses proposed to explain the observed relationships between R_m and M have invoked variation in a range of physical constraints, such as the geometry of circulatory networks[4,5], the need to dissipate heat[7,20], or surface area-to-volume ratios that influence the flux of nutrients or wastes[21–23]. Other approaches that explain variation in metabolic scaling have invoked biotic and abiotic drivers such as lifestyle and temperature[24], foraging[25], predation[26] and a range of others[6–9,27], or differences in body size optimization and the distributions of intraspecific production and mortality parameters across species[28]. Here, we complement these studies by investigating microevolutionary and macroevolutionary processes responsible for variation in the scaling of R_m in animals.

Theory predicts that microevolutionary processes can lead to macroevolutionary associations between R_m and M in at least two ways. (1) Metabolic allometry could arise due to constraints in the genetic architecture of traits, with little to no role for selection coupled with random evolution[29]. When two traits share genetic variance, through pleiotropy, they do not evolve independently[30]; thus, the evolution of R_m and M could be constrained if the two traits are genetically correlated. Under this scenario, a macroevolutionary relationship between R_m and M is expected to arise and persist even in the absence of selection. (2) Metabolic allometry could also arise through correlational selection increasing the covariance between R_m and M[29,31]. Under this model, natural selection favours particular combinations of R_m and M over others, and it is the pattern of multivariate selection that gives rise to the sublinear scaling of R_m with M. This model implies that fitness would differ between individuals with the same mass-specific R_m (R_m/M) and different M; fitness would be highest for small individuals with high mass-specific R_m and for large individuals with low mass-specific R_m.

To distinguish between these two explanations (hereafter, random evolution and correlational selection), we took a three-pronged approach. First, we estimated the distribution and strength of the genetic correlation between R_m and M for a suite of species across 800 Myr of animal evolution. Using the distribution of genetic correlations between R_m and M and the distributions of the genetic variances of these traits, we next simulated repeatedly the evolution of R_m and M along a phylogeny. This process generated a distribution of values for each of these traits, from which we could calculate the variation in both the scaling exponent of R_m and the magnitude of residual variation in R_m (the variation in R_m that is not explained by variation in M). We then compared the distributions of the simulated data with empirical data. If the

[1]School of Biological Sciences, The University of Queensland, Brisbane, Queensland, Australia. [2]Centre for Geometric Biology, School of Biological Sciences, Monash University, Melbourne, Victoria, Australia. [3]Research School of Biology, The Australian National University, Canberra, Australian Capital Territory, Australia. [4]School of Biosciences, The University of Melbourne, Melbourne, Victoria, Australia. [5]School of Life Sciences, Arizona State University, Tempe, AZ, USA. [6]Department of Life Sciences, University of Roehampton, London, UK. [7]School of Biological Sciences, Royal Holloway, University of London, Egham, UK. *e-mail: craig.white@monash.edu

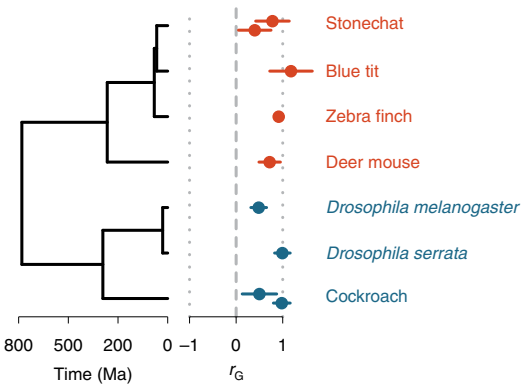

Fig. 1 | Phylogenetic distribution of the genetic correlation (r_G) between R_m and M. Species are (from top to bottom): African stonechat *Saxicola torquata*[32] (estimate for *S. torquata axillaris* plotted above that for *S. torquata rubicola*); blue tit *Cyanistes caeruleus*[33]; zebra finch *Taeniopygia guttata*[34]; deer mouse *Peromyscus maniculatus*[35]; *D. melanogaster*; *D. serrata*; cockroach *N. cinerea* (estimate for females is plotted above that for males). Dotted lines correspond to values of r_G of −1 and +1, while the dashed line corresponds with $r_G = 0$. Data are shown ± s.e. The tree was dated using www.timetree.org. Endothermic species are coloured red, while ectothermic species are coloured blue. Ma, million years ago.

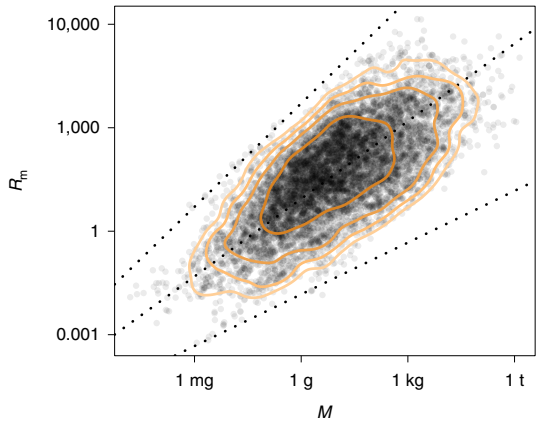

Fig. 2 | Relationship between R_m and M predicted by random evolution. Results are for 4,000 tips evolving on a random tree, with a genetic correlation between R_m and M ($r_G = 0.78$; Fig. 1), a variance of 0.025 for log-transformed M and a variance of 0.0183 for log-transformed R_m, calculated from the mean ratio of $\sigma^2_{R_m}$ to σ^2_M; that is, 0.73 (see text for details). Orange lines are density contours corresponding to (from the inner to outer contour) the 50th, 80th, 90th and 95th percentiles. Dashed lines represent (from top to bottom) scaling exponents of 1, 0.75 and 0.5.

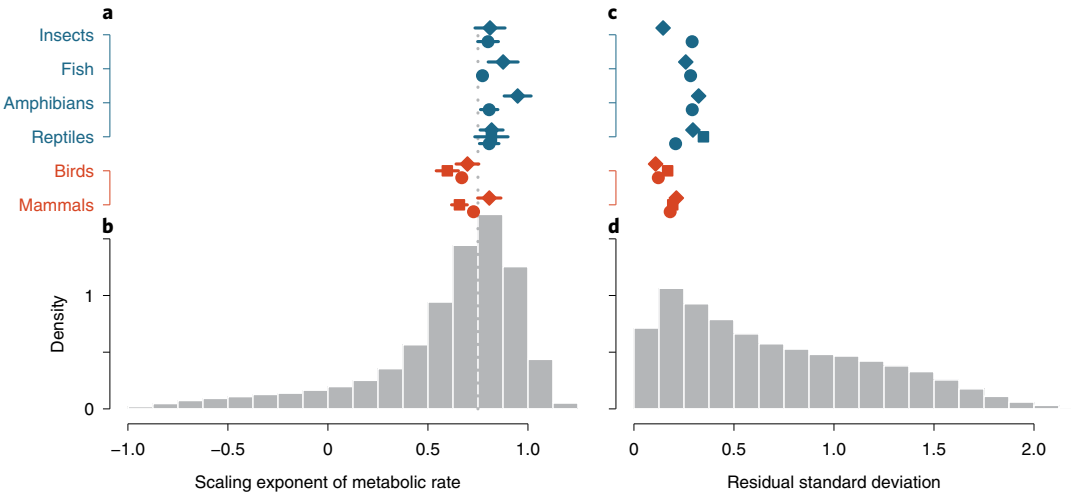

Fig. 3 | Empirical and simulated distributions of metabolic scaling exponents and mass-independent variation in R_m. a, Empirical scaling exponent of R_m for a range of species measured at rest (circles), while free living (squares) or during intense activity (diamonds), shown ± 95% confidence intervals. Groups that are predominantly endothermic are coloured red, while groups that are predominantly ectothermic are coloured blue. **b**, Grey bars depict the distribution of simulated scaling exponents under a model of random evolution with a genetic correlation. The vertical dashed line represents the scaling exponent of ¾ predicted by several metabolic theories[4,5,44,45]. **c**, Standard deviation of the variation in R_m that is not explained by variation in M or temperature (residual variation) for the relationships in **a**. **d**, Standard deviation of the variation in R_m that is not explained by variation in M for the relationships in **b**.

distribution of simulated values of the scaling exponent b and the distribution of simulated residual (mass-independent) variation in R_m both match their empirical distributions, the allometric scaling of R_m with M could have resulted from random evolution. In contrast, if the distribution of simulated values of b does not match the empirical distribution, or if the simulated residual variation of R_m is greater than that of the empirical data, this would show that the allometric scaling of R_m with M is instead consistent with evolution under correlational selection.

Results

As was the case in previous studies of birds[32–34] and mammals[35], our own empirical estimates for three species of insects revealed that the genetic correlation (r_G) between M and resting R_m is positive and strong (Fig. 1). In a previous study of speckled cockroaches *Nauphoeta cinerea*[36], we determined the additive genetic correlation using a paternal half-sibling–full-sibling breeding design ($n = 637$ individuals; 48 half-sibling families and 126 full-sibling families). In a previous study of fruit flies

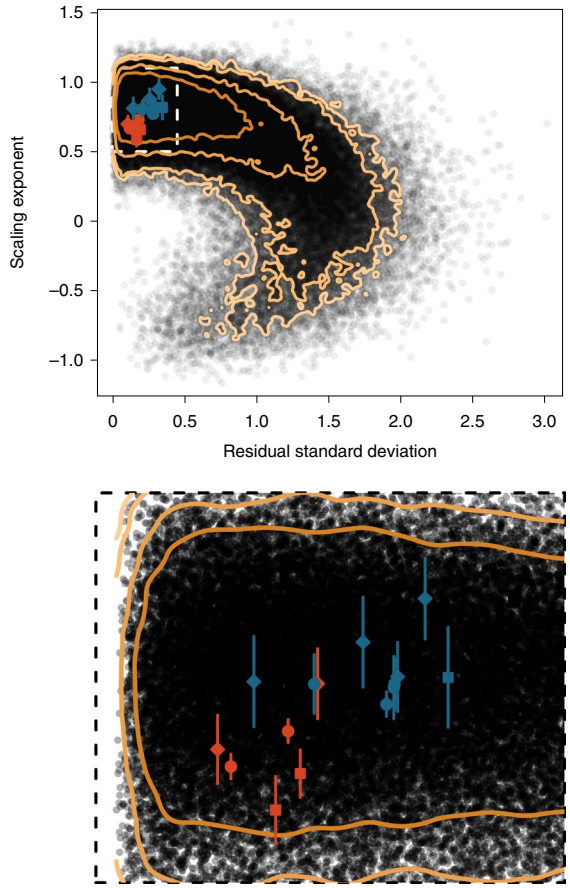

Fig. 4 | Metabolic scaling relationships are not consistent with random evolution under a genetic constraint alone. Top, the black dots depict the combinations of scaling exponents and residual standard deviation that are produced by 100,000 simulations of the evolution of R_m and M by random evolution under a genetic constraint with genetic correlations modelled based on their empirical distribution (see text for details). Orange lines are (inner to outer) 50th, 70th, 90th and 95th percentile density contours of the 100,000 simulated exponents. Red and blue symbols represent empirical metabolic scaling exponents for endotherms and ectotherms, respectively, for animals measured at rest (circles), while free living (squares) or during intense activity (diamonds), shown ± 95% confidence intervals. Bottom, magnified reproduction of the area enclosed by the dashed box in the top panel.

Drosophila melanogaster ($n = 247$ individuals), we measured the R_m and M values of 85 isofemale lines[37]. In the present study, we measured R_m and M values of 438 individual *Drosophila serrata* from 45 isofemale lines created from natural populations. For both species of *Drosophila*, we determined genetic correlations among isofemale lines (see Supplementary Information for details). For all 3 species of insect, a strong positive genetic correlation was observed (*N. cinerea* males: 0.98 ± 0.18 (s.d.); females: 0.50 ± 0.37; *D. melanogaster*: 0.48 ± 0.17; *D. serrata*: 0.99 ± 0.17). For the full dataset, including birds and mammals, r_G values range from 0.40 ± 0.35 to 1.18 ± 0.46 (Fig. 1).

To evaluate theoretical predictions, we first explored whether random evolution could have produced the observed distribution of interspecific scaling exponents (b). We simulated the evolution of R_m and M along phylogenies (for example, Fig. 2), and compared our simulated data with an empirical distribution of b estimated from 4,794 means of R_m and M for 2,168 species. These data include 3,799 of our own measurements of R_m for 2,936 individuals of 32 species, in addition to those compiled from the literature (all data are provided in the Supplementary Information).

The empirical estimates of b for resting, free-living and active animals (Supplementary Fig. 1) fall within the simulated distribution based on the genetic correlation between R_m and M and their genetic variances (Fig. 3a,b). The empirical values for the residual variances also fall within the simulated distribution (Fig. 3c,d). However, the tails of the simulated distributions are long (Fig. 3), and the 95% density contour of the simulated data includes regions of parameter space far outside the narrow region occupied by the empirical data (Fig. 4). The relationship between R_m and M is therefore far more constrained than expected by chance, and we conclude that the macroevolutionary relationship between R_m and M arises as a consequence of correlational selection on these traits. This conclusion is robust to the underlying distribution of the ratio of $\sigma^2_{R_m}$ to σ^2_M used in the simulations (Supplementary Figs. 2–4).

Discussion

Theory predicts that responses to selection on a trait initially depend on the genetic correlations between traits, but they are determined by a balance between the intensities of stabilizing and directional selection over longer time scales[31]. Genetic correlations can arise by chance[38] and as a consequence of multivariate selection[39–41]. We hypothesize that the apparent persistence of the genetic correlation between R_m and M over at least some narrow regions of the tree of life suggests that multivariate selection is probably responsible for the distribution of genetic correlations observed in extant species (Fig. 1). Such multivariate selection acting on R_m and M could also act to constrain the observed distributions of these traits, restricting the empirical distributions of b and residual variances to the narrow range observed relative to simulations (Fig. 4). Genetic correlations can vary among environments[42], as can intraspecific metabolic scaling relationships [6,24,26,43], so comparisons of the genetic (co-) variances of R_m and M for animals reared or evolved in multiple environments would also be valuable and might provide insight into how the strength and direction of multivariate selection varies among environments. Such data may be particularly useful in explaining the shifts in metabolic scaling that are observed across the tree of life[11].

Multivariate selection on R_m and M could result from physical constraints associated with nutrient mobilization[23,44,45], nutrient transport[4,5], heat dissipation[7,20], the exchange of nutrients or wastes across surfaces[21,22], or combinations of these acting on different combinations of R_m and M. Variation in the relative contribution of these physical constraints, or their mediation by environmental context, might also contribute to variation in the scaling exponent of R_m[8,23,44,45]. Yet, despite the considerable interest in these mechanistic hypotheses, variation in these functional characteristics of organisms has not been empirically linked to measurements of fitness, either directly or indirectly via variation in R_m; indeed, measurements of the link between lifetime reproductive success and R_m are exceedingly rare[10]. Future work could fill this knowledge gap by examining how the putative mechanistic drivers of metabolic scaling determine the functional basis of variation in fitness.

Our results show that interspecific relationships between R_m and M in animals are consistent with evolution under persistent multivariate selection. The strong positive genetic correlation between R_m and M is present in species of insect, bird and mammal spanning around 800 Myr of evolution (Fig. 1) and might have arisen as a consequence of persistent multivariate selection. These factors (random evolution, multivariate selection and a persistent genetic correlation) link the micro- and macroevolution of R_m and M, thereby explaining the multivariate distributions of these fundamental traits

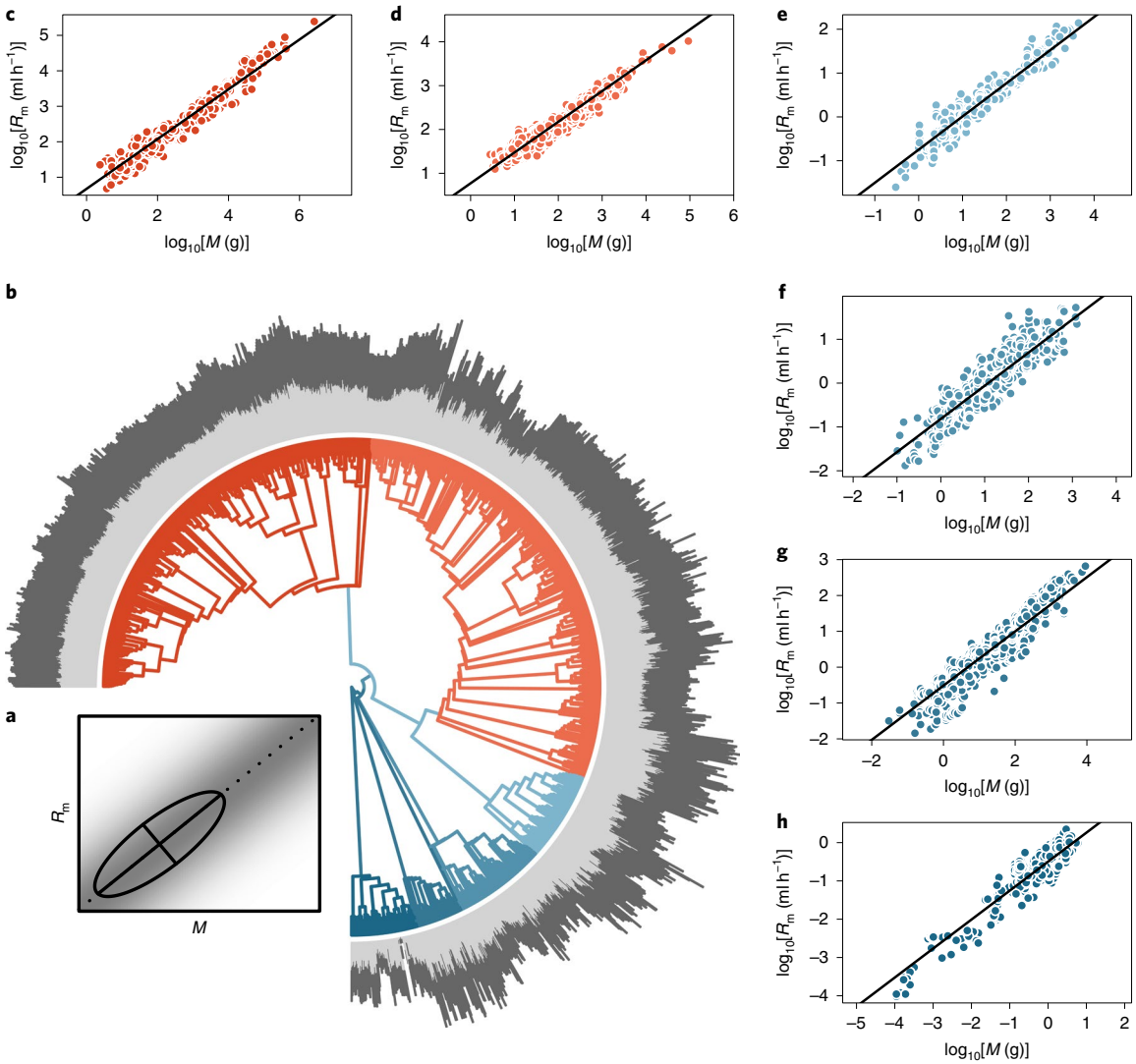

Fig. 5 | Phylogenetic diversity of R_m and M. a, Ellipse outlining the additive genetic ('breeding') values of individuals within a population. The shading depicts the fitness surface (darker shading corresponds with higher fitness) describing the pattern of correlational selection on R_m and M hypothesized to generate the additive genetic correlation between R_m and M, and to constrain the evolution of mass-independent R_m. The long axis of the ellipse is the direction of greatest genetic variance, $\boldsymbol{g}_{max}$, which represents the genetic line of least resistance[61] depicted by the dashed line. **b**, If the additive genetic variance–covariance matrix is stable through time, evolution should proceed along the direction of $\boldsymbol{g}_{max}$ in the absence of selection, yielding strongly correlated phenotypic values of R_m and M, as is observed for extant species (the lengths of the light grey bars are proportional to $\log_{10}$-transformed M, while the lengths of the dark grey bars are proportional to $\log_{10}$-transformed resting R_m). **c**–**h**, The observed additive genetic correlation between R_m and M for a range of animals (Fig. 1) predicts the among-species relationship between R_m and M for mammals (**c**), birds (**d**), reptiles (**e**), amphibians (**f**), fish (**g**) and insects (**h**). The slopes of the solid lines for the scaling of resting R_m values are the median simulated values for endotherms and ectotherms from Fig. 3b. Colours correspond with the clades in **b**.

across the animal tree of life (Fig. 5): microevolutionary processes dictate the trait space available to organisms, and macroevolutionary patterns describe the regions of trait space that are selected over long periods of time.

Methods

Measurements of R_m. R_m values were measured using standard positive pressure flow-through respirometry[46], using techniques that are described in detail elsewhere (for example, refs. [36,37]) and in the supplementary Information. Briefly, air was scrubbed of CO_2 and water vapour before being passed at a known flow rate through a chamber containing an animal, and the concentration of CO_2, or the concentrations of O_2 and CO_2, were measured in the excurrent air. Rates of CO_2 production and O_2 consumption were then calculated using standard equations[46]. For systems in which only CO_2 was measured, rates of CO_2 production were converted to rates of O_2 consumption assuming a respiratory exchange ratio of 0.8 (that is, the rate of CO_2 production divided by the rate of O_2 production).

Determination of genetic correlations. For *D. serrata*, genetic (among-line) correlations between M and R_m—conditioned on activity and age[48]—were calculated using ASReml-R version 3.0 (ref. [49]) in R version 2.0.2. Approximate standard errors for the estimate of the genetic correlation were calculated using the R 'pin' function[47]. For *D. melanogaster*, genetic (among-line) correlations between M and R_m—conditioned on temporal block, population and measurement temperature[48]—were calculated.

Simulations of trait evolution. We simulated the evolution of $\log_{10}[M]$ and $\log_{10}[R_m]$ over randomly generated phylogenies with 4,000 tips using the 'pbtree' function of the phytools[48] package in R[49]. Preliminary analyses showed that the results were qualitatively similar when larger trees were used, but the processing time was considerably increased. We therefore selected a value of 4,000 tips because

it is similar to the number of extant species of mammal. The results were also similar if a real tree with branch lengths in units of time was used[50]. We simulated trait values using the 'sim.corrs' function of phytools to conduct Brownian motion simulation on a tree with evolutionary correlations between characters[48]. We set the starting values for the simulation as the medians of $\log_{10}$-transformed M and basal R_m for mammals[51]; the simulated distributions of b and mass-independent R_m are unaffected by these starting values, which influence only the means of $\log_{10}[M]$ and $\log_{10}[R_m]$ for the simulated data, not their (co)variances. We set the variance for $\log_{10}[M]$ (σ^2_M) at 0.025 to yield simulated body masses for extant taxa at the tip of the tree that span a biologically realistic range. We calculated the variance for $\log_{10}[R_m]$ ($\sigma^2_{R_m}$) based on a distribution of 100,000 values generated using a Weibull distribution (shape = 3.23; scale = 0.818) fitted to the empirical distribution of 4 values of the ratio of $\sigma^2_{R_m}$ to σ^2_M calculated using log-transformed data for *D. serrata* (0.81), *D. melanogaster* (0.55), and male and female *N. cinerea* (1.1 and 0.47, respectively). We set covariances at $r_G\sqrt{\sigma^2_{R_m}}\sqrt{\sigma^2_M}$, where we generated a distribution of 100,000 values of r_G based on the distribution of Fisher's Z-transformed values of r_G for extant species (mean $Z = 1.55$; s.d. = 1.18; $n = 9$; for Z-transformation, estimates of $r_G \geq 1$ were substituted with values of 0.999; there was no systematic difference between estimates of Z calculated using log-transformed or untransformed data ($t_7 = 0.156$; $P = 0.86$), so all data were pooled). In each simulation, traits evolved randomly by Brownian motion along the tree (for example, Fig. 2), and we replicated the simulation 100,000 times.

Compilation of comparative data for M and R_m. To test the predictions of our simulations, we assembled a database of M and R_m data, which includes measurements of resting animals (basal R_m[52] for birds and mammals; standard R_m[52] for insects, fish, amphibians and reptiles), free-living animals (daily energy expenditure[53] for reptiles, birds and mammals) and animals exercising at or near their aerobic limits in a laboratory setting (maximum aerobic R_m[54] for terrestrial mammals and cursorial birds; maximum rate of oxygen uptake for fish[55]; and R_m during flight for insects, bats and birds). In addition to our measurements of R_m (Supplementary Table 1), we assembled published databases and generated new compilations where published databases were not available (Supplementary Table 2).

For our new compilations of insect standard R_m (Supplementary Table 3) and flight R_m (Supplementary Table 4), reptile field R_m (Supplementary Table 5), and bird field R_m (Supplementary Table 6) and maximum R_m (Supplementary Table 7), we searched online databases (Google Scholar and Web of Science) using key words that identified the measurements of interest ('metabolic rate' or 'rate of oxygen consumption' or 'rate of carbon dioxide production' or 'respirometry' or 'calorimetry' or 'doubly labelled water' or 'daily energy expenditure' or 'aerobic capacity'). For each of the records identified by this search, we first scanned the title to determine whether a record was likely to contain data or citations to data. If the title was promising, we reviewed the abstract, and if that was promising we reviewed the full text. For each record that was reviewed at the full-text level, we also searched for cited papers that might contain data. Unfortunately, we did not maintain a tally of how many records were retrieved or how many papers were reviewed at each level. The full database of R_m values includes species that vary in size from ants to elephants (0.1 mg–2.6 Mg). R_m values ranged from 35 pl min^{-1} of O_2 for resting weevils (0.5 mg) to 3.6 l min^{-1} of O_2 for exercising horses (450 kg).

Determination of empirical scaling exponents. We calculated the scaling exponent of R_m, b, for each taxonomic group (insects, fish, amphibians, reptiles, birds and mammals) and each metabolic state (resting, free living and exercising) using phylogenetic mixed models[58–60] with phylogenetic relationships from version 3 of the Open Tree of Life[59]. We implemented phylogenetic mixed models using ASReml-R version 3.0 (ref. [49]) and R version 3.0.2, with inverse relatedness matrices calculated from phylogenetic covariance matrices using the MCMCglmm package version 2.21 (ref. [60]). Models for endotherms and free-living reptiles included $\log_{10}[R_m]$ as a response and $\log_{10}[M]$ as a predictor, and all other models for ectotherms included $\log_{10}[R_m]$ as a response and both $\log_{10}[M]$ and measurement temperature as predictors. The parameter estimate for $\log_{10}[M]$ in each of these models represents the scaling exponent of R_m[9].

Reporting Summary. Further information on research design is available in the Nature Research Reporting Summary linked to this article.

Data availability

All data generated or analysed during this study are included within the article and its supplementary Information files.

Received: 13 December 2017; Accepted: 5 February 2019;
Published online: 18 March 2019

References

1. Vernon, H. M. The physiological evolution of the warm-blooded animal. *Sci. Prog.* **7**, 378–394 (1898).
2. Krogh, A. *Respiratory Exchange of Animals and Man* (Longmans, Green and Co., London, 1916).
3. Schmidt-Nielsen, K. *Scaling: Why is Animal Size so Important?* (Cambridge Univ. Press, Cambridge, 1984).
4. West, G. B., Brown, J. H. & Enquist, B. J. A general model for the origin of allometric scaling laws in biology. *Science* **276**, 122–126 (1997).
5. West, G. B., Brown, J. H. & Enquist, B. J. The fourth dimension of life: fractal geometry and allometric scaling of organisms. *Science* **284**, 1677–1679 (1999).
6. Glazier, D. S. Beyond the '3/4-power law': variation in the intra- and interspecific scaling of metabolic rate in animals. *Biol. Rev.* **80**, 611–662 (2005).
7. Glazier, D. S. A unifying explanation for diverse metabolic scaling in animals and plants. *Biol. Rev.* **85**, 111–138 (2010).
8. White, C. R. & Kearney, M. R. Determinants of inter-specific variation in basal metabolic rate. *J. Compr. Physiol. B* **183**, 1–26 (2013).
9. White, C. R. & Kearney, M. R. Metabolic scaling in animals: methods, empirical results, and theoretical explanations. *Compr. Physiol.* **4**, 231–256 (2014).
10. Pettersen, A. K., Marshall, D. J. & White, C. R. Understanding variation in metabolic rate. *J. Exp. Biol.* **221**, jeb166876 (2018).
11. Uyeda, J. C., Pennell, M. W., Miller, E. T., Maia, R. & McClain, C. R. The evolution of energetic scaling across the vertebrate tree of life. *Am. Nat.* **190**, 185–199 (2017).
12. Brown, J. H., Gillooly, J. F., Allen, A. P., Savage, V. M. & West, G. B. Toward a metabolic theory of ecology. *Ecology* **85**, 1771–1789 (2004).
13. Burton, T., Killen, S. S., Armstrong, J. D. & Metcalfe, N. B. What causes intraspecific variation in resting metabolic rate and what are its ecological consequences? *Proc. R. Soc. Lond. B* **278**, 3465–3473 (2011).
14. Biro, P. A. & Stamps, J. A. Do consistent individual differences in metabolic rate promote consistent individual differences in behavior? *Trends Ecol. Evol.* **25**, 653–659 (2010).
15. Pettersen, A. K., White, C. R. & Marshall, D. J. Metabolic rate covaries with fitness and the pace of the life history in the field. *Proc. R. Soc. Lond. B* **283**, 20160323 (2016).
16. McNab, B. K. Ecological factors affect the level and scaling of avian BMR. *Comp. Biochem. Physiol. A* **152**, 22–45 (2009).
17. McNab, B. K. An analysis of the factors that influence the level and scaling of mammalian BMR. *Comp. Biochem. Physiol. A* **151**, 5–28 (2008).
18. Kolokotrones, T., Savage, V. M., Deeds, E. J. & Fontana, W. Curvature in metabolic scaling. *Nature* **464**, 753–756 (2010).
19. White, C. R., Phillips, N. F. & Seymour, R. S. The scaling and temperature dependence of vertebrate metabolism. *Biol. Lett.* **2**, 125–127 (2006).
20. Speakman, J. R. & Król, E. Maximal heat dissipation capacity and hyperthermia risk: neglected key factors in the ecology of endotherms. *J. Anim. Ecol.* **79**, 726–746 (2010).
21. Speakman, J. R., McDevitt, R. M. & Cole, K. R. Measurement of basal metabolic rates: don't lose sight of reality in the quest for comparability. *Physiol. Zool.* **66**, 1045–1049 (1993).
22. Hirst, A. G., Glazier, D. S. & Atkinson, D. Body shape shifting during growth permits tests that distinguish between competing geometric theories of metabolic scaling. *Ecol. Lett.* **17**, 1274–1281 (2014).
23. Kooijman, S. A. L. M. *Dynamic Energy Budget Theory for Metabolic Organisation* 3rd edn (Cambridge Univ. Press, Cambridge, 2010).
24. Killen, S. S., Atkinson, D. & Glazier, D. S. The intraspecific scaling of metabolic rate with body mass in fishes depends on lifestyle and temperature. *Ecol. Lett.* **13**, 184–193 (2010).
25. Witting, L. The body mass allometries as evolutionarily determined by the foraging of mobile organisms. *J. Theor. Biol.* **177**, 129–137 (1995).
26. Glazier, D. S. et al. Ecological effects on metabolic scaling: amphipod responses to fish predators in freshwater springs. *Ecol. Monogr.* **81**, 599–618 (2011).
27. Glazier, D. S. Is metabolic rate a universal 'pacemaker' for biological processes?. *Biol. Rev.* **90**, 377–407 (2015).
28. Kozłowski, J. & Weiner, J. Interspecific allometries are by-products of body size optimization. *Am. Nat.* **149**, 352–380 (1997).
29. Lande, R. Quantitative genetic analysis of multivariate evolution, applied to brain:body size allometry. *Evolution* **33**, 402–416 (1979).
30. Walsh, B. & Blows, M. W. Abundant genetic variation + strong selection = multivariate genetic constraints: a geometric view of adaptation. *Annu. Rev. Ecol. Evol. Syst.* **40**, 41–59 (2009).
31. Zeng, Z.-B. Long-term correlated response, interpopulation covariation, and interspecific allometry. *Evolution* **42**, 363–374 (1988).
32. Tieleman, B. I., Versteegh, M. A., Helm, B. & Dingemanse, N. J. Quantitative genetics parameters show partial independent evolutionary potential for body mass and metabolism in stonechats from different populations. *J. Zool.* **278**, 129–136 (2009).
33. Nilsson, J.-Å., Åkesson, M. & Nilsson, J. F. Heritability of resting metabolic rate in a wild population of blue tits. *J. Evol. Biol.* **22**, 1867–1874 (2009).
34. Ronning, B., Jensen, H., Moe, B. & Bech, C. Basal metabolic rate: heritability and genetic correlations with morphological traits in the zebra finch. *J. Evol. Biol.* **20**, 1815–1822 (2007).

35. Careau, V. et al. Genetic correlation between resting metabolic rate and exploratory behaviour in deer mice (*Peromyscus maniculatus*). *J. Evol. Biol.* **24**, 2153–2163 (2011).
36. Schimpf, N. G., Matthews, P. G. D. & White, C. R. Discontinuous gas exchange exhibition is a heritable trait in speckled cockroaches *Nauphoeta cinerea*. *J. Evol. Biol.* **26**, 1588–1597 (2013).
37. Alton, L. A., Condon, C., White, C. R. & Angilletta, M. J. Jr. Colder environments did not select for a faster metabolism during experimental evolution of *Drosophila melanogaster*. *Evolution* **71**, 145–152 (2017).
38. Nespolo, R. F. & Roff, D. A. Testing the aerobic model for the evolution of endothermy: implications of using present correlations to infer past evolution. *Am. Nat.* **183**, 74–83 (2014).
39. Delph, L. F., Steven, J. C., Anderson, I. A., Herlihy, C. R. & Brodie, E. D. III Elimination of a genetic correlation between the sexes via artificial correlational selection. *Evolution* **65**, 2872–2880 (2011).
40. Roff, D. A. & Fairbairn, D. J. A test of the hypothesis that correlational selection generates genetic correlations. *Evolution* **66**, 2953–2960 (2012).
41. Roff, D. A. & Fairbairn, D. J. The evolution of trade-offs under directional and correlational selection. *Evolution* **66**, 2461–2474 (2012).
42. Sgrò, C. M. & Hoffmann, A. A. Genetic correlations, tradeoffs and environmental variation. *Heredity* **93**, 241–248 (2004).
43. Glazier, D. S. The 3/4-power law is not universal: evolution of isometric, ontogenetic metabolic scaling in pelagic animals. *Bioscience* **56**, 325–332 (2006).
44. Kooijman, S. A. L. M. Energy budgets can explain body size relations. *J. Theor. Biol.* **121**, 269–282 (1986).
45. Maino, J. L., Kearney, M. R., Nisbet, R. M. & Kooijman, S. A. L. M. Reconciling theories for metabolic scaling. *J. Anim. Ecol.* **83**, 20–29 (2014).
46. Lighton, J. R. B. *Measuring Metabolic Rates: A Manual for Scientists* (Oxford Univ. Press, Oxford, 2008).
47. Wilson, A. J. Why h^2 does not always equal V_A/V_P? *J. Evol. Biol.* **21**, 647–650 (2008).
48. Gilmour, A. R. et al. *ASReml User Guide Release 3.0* (NSW Department of Industry and Investment, 2009).
49. White, I. Pin function for ASReml-R. http://www.homepages.ed.ac.uk/iwhite//asreml/ (2013).
50. Revell, L. J. phytools: an R package for phylogenetic comparative biology (and other things). *Methods Ecol. Evol.* **3**, 217–223 (2012).
51. R Development Core Team *R: A Language and Environment for Statistical Computing* (R Foundation for Statistical Computing, Austria, 2016).
52. Bininda-Emonds, O. R. P. et al. The delayed rise of present-day mammals. *Nature* **446**, 507–512 (2007).
53. Jones, K. E. et al. PanTHERIA: a species-level database of life history, ecology, and geography of extant and recently extinct mammals. *Ecology* **90**, 2648 (2009).
54. Frappell, P. B. & Butler, P. J. Minimal metabolic rate, what it is, its usefulness, and its relationship to the evolution of endothermy: a brief synopsis. *Physiol. Biochem. Zool.* **77**, 865–868 (2004).
55. Butler, P. J., Green, J. A., Boyd, I. L. & Speakman, J. R. Measuring metabolic rate in the field: the pros and cons of the doubly labelled water and heart rate methods. *Funct. Ecol.* **18**, 168–183 (2004).
56. Dlugosz, E. M. et al. Phylogenetic analysis of mammalian maximal oxygen consumption during exercise. *J. Exp. Biol.* **216**, 4712–4721 (2013).
57. Norin, T. & Clark, T. D. Measurement and relevance of maximum metabolic rate in fishes. *J. Fish Biol.* **88**, 122–151 (2016).
58. Lynch, M. Methods for the analysis of comparative data in evolutionary biology. *Evolution* **45**, 1065–1080 (1991).
59. Housworth, E. A., Martins, E. P. & Lynch, M. The phylogenetic mixed model. *Am. Nat.* **163**, 84–96 (2004).
60. Hadfield, J. D. & Nakagawa, S. General quantitative genetic methods for comparative biology: phylogenies, taxonomies and multi-trait models for continuous and categorical characters. *J. Evol. Biol.* **23**, 494–508 (2010).
61. Hinchliff, C. E. et al. Synthesis of phylogeny and taxonomy into a comprehensive tree of life. *Proc. Natl Acad. Sci. USA* **112**, 12764–12769 (2015).
62. Hadfield, J. D. MCMC methods for multi-response generalized linear models: the MCMCglmm R package. *J. Stat. Softw.* **33**, 1–22 (2010).
63. Schluter, D. Adaptive radiation along genetic lines of least resistance. *Evolution* **50**, 1766–1774 (1996).

Acknowledgements

This research was supported by the Australian Research Council (projects DP110101776, FT130101493, DP170101114 and DP180103925).

Author contributions

C.R.W., D.O.-B. and D.J.M. designed the study. C.R.W., L.A.A., P.A.A., J.E.B., C.L.B., C.C., T.S.C., A.J., E.P., H.S.W.-S., M.J.A., S.F.C., C.E.F., L.G.H., M.R.K. and S.J.P. collected the data. C.R.W. analysed the data. C.R.W. and D.O.-B. wrote the first version of the manuscript. All authors contributed to and approved the final version.

Competing interests

The authors declare no competing interests.

Additional information

Supplementary information is available for this paper at https://doi.org/10.1038/s41559-019-0839-9.

Reprints and permissions information is available at www.nature.com/reprints.

Correspondence and requests for materials should be addressed to C.R.W.

Publisher's note: Springer Nature remains neutral with regard to jurisdictional claims in published maps and institutional affiliations.

nature research

Corresponding author(s): Craig R. White

Last updated by author(s): 2 Feb 2019

Reporting Summary

Nature Research wishes to improve the reproducibility of the work that we publish. This form provides structure for consistency and transparency in reporting. For further information on Nature Research policies, see Authors & Referees and the Editorial Policy Checklist.

Statistics

For all statistical analyses, confirm that the following items are present in the figure legend, table legend, main text, or Methods section.

n/a	Confirmed
☐	☒ The exact sample size (*n*) for each experimental group/condition, given as a discrete number and unit of measurement
☐	☒ A statement on whether measurements were taken from distinct samples or whether the same sample was measured repeatedly
☐	☒ The statistical test(s) used AND whether they are one- or two-sided *Only common tests should be described solely by name; describe more complex techniques in the Methods section.*
☐	☒ A description of all covariates tested
☐	☒ A description of any assumptions or corrections, such as tests of normality and adjustment for multiple comparisons
☐	☒ A full description of the statistical parameters including central tendency (e.g. means) or other basic estimates (e.g. regression coefficient) AND variation (e.g. standard deviation) or associated estimates of uncertainty (e.g. confidence intervals)
☐	☒ For null hypothesis testing, the test statistic (e.g. *F*, *t*, *r*) with confidence intervals, effect sizes, degrees of freedom and *P* value noted *Give P values as exact values whenever suitable.*
☒	☐ For Bayesian analysis, information on the choice of priors and Markov chain Monte Carlo settings
☒	☐ For hierarchical and complex designs, identification of the appropriate level for tests and full reporting of outcomes
☒	☐ Estimates of effect sizes (e.g. Cohen's *d*, Pearson's *r*), indicating how they were calculated

Our web collection on statistics for biologists contains articles on many of the points above.

Software and code

Policy information about availability of computer code

Data collection	Data were collected using ADInstruments LabChart software, as described in the methods.
Data analysis	Data were analysed using publically available R software and packages, as described in the methods.

For manuscripts utilizing custom algorithms or software that are central to the research but not yet described in published literature, software must be made available to editors/reviewers. We strongly encourage code deposition in a community repository (e.g. GitHub). See the Nature Research guidelines for submitting code & software for further information.

Data

Policy information about availability of data

All manuscripts must include a data availability statement. This statement should provide the following information, where applicable:

- Accession codes, unique identifiers, or web links for publicly available datasets
- A list of figures that have associated raw data
- A description of any restrictions on data availability

All data generated or analysed during this study are included in this published article (and its supplementary information files).

Field-specific reporting

Please select the one below that is the best fit for your research. If you are not sure, read the appropriate sections before making your selection.

☒ Life sciences ☐ Behavioural & social sciences ☐ Ecological, evolutionary & environmental sciences

For a reference copy of the document with all sections, see nature.com/documents/nr-reporting-summary-flat.pdf

Life sciences study design

All studies must disclose on these points even when the disclosure is negative.

Sample size	Sample sizes were not pre-determined. Sample sizes for quantitative genetic studies were as large as practically possible given equipment limitations (and are reported in the manuscript). Sample sizes for comparative analyses were limited by the available published data.
Data exclusions	No data were excluded.
Replication	No attempts were made to replicate the three quantitative genetic studies.
Randomization	Animals were selected at random for quantitative genetic analyses; dams were randomly allocated to sires for the half sib-full sib breeding design.
Blinding	No treatment groups were applied, and so blinding was not employed.

Reporting for specific materials, systems and methods

We require information from authors about some types of materials, experimental systems and methods used in many studies. Here, indicate whether each material, system or method listed is relevant to your study. If you are not sure if a list item applies to your research, read the appropriate section before selecting a response.

Materials & experimental systems

n/a	Involved in the study
☒	☐ Antibodies
☒	☐ Eukaryotic cell lines
☒	☐ Palaeontology
☐	☒ Animals and other organisms
☒	☐ Human research participants
☒	☐ Clinical data

Methods

n/a	Involved in the study
☒	☐ ChIP-seq
☒	☐ Flow cytometry
☒	☐ MRI-based neuroimaging

Animals and other organisms

Policy information about studies involving animals; ARRIVE guidelines recommended for reporting animal research

Laboratory animals	The study did not involve laboratory animals.
Wild animals	Adult bees Bombus terrestris were collected by hand at multiple locations in the UK (Alwinton, Lyndhurst, Roehampton, Ambleside, Banbury, and Manchester). Lizards Carlia longipes, Liopholis striata, Liopholis inornata, and Egernia cunninghami, and frogs Litoria nigrofrenata and Platyplectrum ornatum were collected by hand at various locations in Australia. Hedge grasshoppers Valanga irregularis and cowboy beetles Chondropyga dorsalis were collected by hand in suburban Brisbane. Founding populations of Drosophila serrata were established from animals collected along the east coast of Australia: Cooktown, Cardwell, Airlie Beach, Yeppoon, and Brisbane.
Field-collected samples	The study did not involve samples collected in the field.
Ethics oversight	The research was approved by the Queensland Government Department of Environment and Heritage Protection (WISP15016214, WISP10698712), The Government of Western Australia Department of Environment and Conservation (Licence SF008358) and the Victoria Department of Sustainability and Environment (Permit 10005993). Experimental procedures were approved by the University of Queensland NEWMA Animal Ethics Committee (Approval Number SBS/226/14/ARC) and the University of Melbourne (Ethics ID 1112194).

Note that full information on the approval of the study protocol must also be provided in the manuscript.